MODELING OF A TURBULENT ETHYLENE/AIR JET FLAME USING HYBRID FINITE VOLUME/MONTE CARLO METHODS

Ranjan S. Mehta, Anquan Wang*,Michael F. Modestand Daniel C. Haworth**

Department of Mechanical and Nuclear Engineering,
The Pennsylvania State University,
University Park, Pennsylvania 16802, USA
∗GE Global Research Center,
One Research Circle,
Niskayuna, NY 12309, USA.
∗∗ Correspondence Author, Email:mfm@engr.psu.edu

ABSTRACT Detailed modeling of an experimental ethylene/air jet flame is undertaken using the composition PDF method for gas-phase kinetics coupled with detailed models for soot formation and radiation from the flames. The gas-phase kinetics is modeled using a reduced mechanism for ethylene consisting of 33 species and 205 elementary reactions. The soot formation is modeled using the method of moments with a simplified nucleation mechanism and modified surface-HACA mechanism for surface growth and oxidation. The soot formation is coupled directly with a transported PDF approach to account for turbulence–chemistry interactions in gas-phase chemistry and the highly nonlinear soot formation processes. Radiation from soot and combustion gases is accounted for by using a photon Monte Carlo method coupled with nongray properties for soot and gases. Soot particles are assumed to be small, and scattering effects are neglected. Turbulence–radiation interactions are captured accurately. Simulation results are compared with experimental data, and also with less CPU-intensive radiation calculations using the optically thin approximation.

INTRODUCTION

Radiation is a dominant mode of heat transfer in many combustion systems. In numerical simulations, accurate treatment of radiative heat transfer is essential to predict flame structure correctly, which includes temperature, species and particulate matter (soot) distributions inside the flames. Most combustion devices operate in turbulent flow conditions, where turbulence–chemistry interactions (TCI) arise due to highly nonlinear coupling between temperature, species mass fractions and reaction kinetics. Much effort has been dedicated to accurately predict TCI, which remains the main goal of turbulent combustion modeling [Veynante & Vervisch 2002]. Turbulence–radiation interactions (TRI) arise from the highly nonlinear coupling between temperature and composition fluctuations, which cause fluctuations in radiative intensity. The effects of TRI can be comparable to those of TCI in both luminous and nonluminous flames [Cox 1977, Song & Viskanta 1987, Faeth, Gore, Chuech & Jeng 1989].

TRI has started to receive attention in recent years [Song & Viskanta 1987, Li & Modest 2002, Coelho 2007]. It has been shown that accounting for TRI can increase radiative losses from a flame by more than a factor of two [Faeth et al. 1989, Li & Modest 2002] even in nonluminous flames. Advances have been made in accurately capturing TRI in reacting flows using transported PDF methods [Mazumder & Modest 1999, Li & Modest 2002, Tessé, Dupoirieux & Taine 2004, Wang & Modest 2007*b*]. Recently Wang and Modest [2007*b*] developed an advanced Photon Monte Carlo method for spectral radiative calculations, applied to reacting and nonreacting flows. The method uses accurate line-by-line absorption coefficients for combustion gases like CO_2 and H_2O and has been extended to include

nongray radiation due to soot. This method allows capture of TRI arising from correlations between absorption coefficient and local Planck function (emission TRI) and also between absorption coefficient and incident radiation (absorption TRI).

PHYSICAL AND NUMERICAL MODELS

Gas-phase Kinetics A systematically reduced 33 species ethylene mechanism containing 205 elementary reactions is used to model gas-phase kinetics [Law 2005]. The molecular transport properties and thermochemistry have been implemented using TRANSPORT [Kee, Dixon-Lewis, Warnatz, Coltrin & Miller 1986] and CHEMKIN-II [Kee, Rupley & Miller 1989], respectively, and interfaced seamlessly with the underlying CFD code [Zhang & Haworth 2004].

Soot Model Soot emission can dominate gas radiation by more than a factor of ten when soot is present at ppm levels [Modest 2003]. It has been shown that, in the presence of soot, peak temperatures can drop by more than 300K due to soot radiation [Bandaru 2000]. Thus accurate prediction of soot levels is essential when modeling sooting flames. In addition, the temperature field affects kinetic rates of most gas-phase reactions and soot-subprocesses, thereby changing the flame structure significantly.
Detailed and semi-detailed soot models generally have two parts: i) soot kinetics (interaction between soot particles and the surrounding gas-phase species) that includes nucleation, surface growth and oxidation models; and ii) soot-particle dynamics (interaction between the soot particles) that includes coagulation and aggregation. The soot particle dynamics can be treated in different ways. These include the method of moments where one solves for the moments of the particle-size distribution function (PSDF) [Frenklach 2002], or sectional methods [McEnally, Schaffer, Long, Pfefferle, Smooke, Colket & Hall 1998] where the PSDF is divided into discrete sections by average particle size. Here a method of moments with interpolative closure has been used. Three to six moments have been found to be sufficient in previous modeling studies of laminar premixed flames [Frenklach & Wang 1994, Appel, Bockhorn & Frenklach 2000] and opposed-flow diffusion flames [Wang, Du, Sung & Law 1996]. The method of moments can be extended to aggregation of soot particles into mass fractals [Kazakov & Frenklach 1998]. Since the current study is limited to atmospheric-pressure flames, it is expected that soot particles will remain primarily spheroidal; hence aggregation is not considered.

Soot kinetics. Soot formation is a complex process and can be divided into several subprocesses: i) nucleation of soot particles, when they acquire characteristics different from the gas-phase; ii) surface growth/oxidation of soot particles due to reactions with the gas-phase and iii) particle coagulation/aggregation due to collisions with each other. All these processes occur simultaneously and need to be modeled accurately [Bockhorn 1994]. Much research has been done in past decades on the nature of soot nucleation, and many models have been put forth [Kennedy 1997]. It is generally accepted that soot particles are nucleated after formation of large polycyclic aromatic hydrocarbon (PAH) molecules. However, nucleation models based on large molecules require these to be included in the gas-phase thermochemistry [Frenklach & Wang 1994], resulting in large gas-phase mechanisms containing hundreds of species [Appel et al. 2000]. These large mechanisms are computationally prohibitive for simulating turbulent flames and alternative models are of interest. In the case of non-premixed flames burning in atmospheric conditions, it has been observed that most contributions to

soot mass are due to surface reactions and are relatively insensitive to nucleation models [Leung, Lindstedt & Jones 1991, Mehta, Haworth & Modest 2008]. Here a simplified nucleation mechanism based on local acetylene (C_2H_2) concentration proposed by Leung, Lindstedt and Jones [1991] has been used; this has been shown to work well in turbulent flames as well [Lindstedt & Louloudi 2005, Mehta, Haworth & Modest 2007].

Soot surface growth models have been an active area of research for several decades [Kennedy 1997]. Frenklach and Wang [1991, 1994] proposed chemical similarity, which postulates that chemical reactions taking place on the soot particle surface are analogous to those for large PAH molecules [Frenklach & Wang 1991]. The surface-HACA mechanism is consistent with the findings of Harris and Weiner [1985], who determined that acetylene dominates surface growth in their flames. Soot surface oxidation is due to attack by OH radicals and oxygen [Neoh, Howard & Sarofim 1981]. Here the surface-HACA mechanism has been used [Frenklach & Wang 1994]. The key reactions involved in surface growth/oxidation of soot particles are listed in Table 1.

Table 1. Surface Growth Mechanism

No.	Reaction	References
1	$C_s + \mathrm{H} \leftrightarrows C_s^* + \mathrm{H_2}$	[Frenklach & Wang 1994, Appel et al. 2000]
2	$C_s + \mathrm{OH} \leftrightarrows C_s^* + \mathrm{H_2O}$	[Frenklach & Wang 1994, Appel et al. 2000]
3	$C_s^* + \mathrm{H} \rightarrow C_s$	[Frenklach & Wang 1994]
4*A*	$C_s + \mathrm{C_2H_2} \rightarrow C_s + \mathrm{H}$	[Frenklach & Wang 1994]
4*B*	$C_s + \mathrm{C_2H_2} \rightarrow C_s^* + \mathrm{H}$	[Wang et al. 1996]
5	$C_s^* + \mathrm{O_2} \rightarrow 2\mathrm{CO} + \mathrm{products}$	[Frenklach & Wang 1994]
6	$C_s + \mathrm{OH} \rightarrow \mathrm{CO} + \mathrm{products}$	[Neoh et al. 1981, Frenklach & Wang 1994]

Here $\rightarrow$ indicates an irreversible reaction and $\leftrightarrows$ denotes a reversible reaction, C_s denotes a soot particle and C_s^* is a soot radical. The kinetic rate coefficients for each of the reactions and other details can be found in the references listed in the table.

Soot particle dynamics. The time evolution of a particle ensemble is described by population balance equations known as the "Smoluchowski master equations" [Fuchs 1989, Seinfeld & Pandis 1998]. These can be written as,

$$\frac{dN_1}{dt} = -\sum_{j=1}^{\infty} \beta_{1,j} N_1 N_j \tag{1a}$$

$$\frac{dN_i}{dt} = \frac{1}{2}\sum_{j=1}^{i-1} \beta_{j,i-j} N_j N_{i-j} - \sum_{j=1}^{\infty} \beta_{i,j} N_i N_j \qquad i = 2\ldots\infty. \tag{1b}$$

Here N_i denotes the number of particles of size i per unit volume: i.e., size i particle number density. N_1 is the number density of the smallest particles and $\beta_{i,j}$ is the collision coefficient between particles of size i and j. In general, then, $\beta_{i,j} = \beta_{i,j}(N_i, N_j, m_i, m_j)$ where m_i is the mass of particle of size i.

The concentration moment of the particle number density function N_i is

$$M_r = \sum_{i=1}^{\infty} m_i^r N_i. \tag{2}$$

It can be seen that if $r = 0$, then $M_0 = \sum_{i=1}^{\infty} N_i$ is the total particle number density. For $r = 1$, $M_1 = \sum_{i=1}^{\infty} m_i N_i$ is the total mass of particles per unit volume, so that the volume fraction is given by $f_v = M_1/\rho_s$, where ρ_s is the density of soot particles. Higher order moments may lack a simple physical interpretation but are needed for accuracy. It can be seen that knowledge of all integer moments ($r = 0, \ldots, \infty$) is equivalent to knowledge of the size distribution function itself. However, most of the principal properties for the particle ensemble can be deduced from the first few moments.
Nucleation, surface growth and particle coagulation equations are then cast in those for the moments of the PSDF in the following form.

$$\frac{dM_r}{dt} = R_r + G_r + W_r \qquad r = 0, 1, \ldots M_{\max}. \tag{3}$$

where R_r is source due to nucleation, G_r due to coagulation, W_r due to surface reactions and $M_{\max}$ is the number of moments retained in the formulation. Unclosed terms appearing in these equations are closed using an interpolative closure whose details can be found in Frenklach [2002]. Here $M_{\max} = 5$ is used and is expected to suffice. At higher pressures, soot coagulation results in formation of mass fractals that have geometries far from spheroidal [Kazakov & Frenklach 1998]. However, since the current study is limited to atmospheric-pressure flames, it is expected that soot particles will stay mainly small and spheroidal. This assumption was found to be sufficient in turbulent flames simulated by Lindstedt and Louloudi [2005]. Soot coagulation is considered in free-molecular, continuum and transition regimes. The surface reaction rate due to gaseous species (growth or oxidation) for a soot moment r can be written as,

$$W_r^{surf} = k_{sg} C_g \alpha \chi_s M_0 \sum_{k=0}^{r-1} \binom{r}{k} \Delta m^{r-k} \mu_{r+2/3} \tag{4}$$

where k_{sg} is the kinetic rate coefficient for reaction with gas g, C_g is the molar concentration of the gas species, α is a steric factor, χ_s is the nominal number density of surface radical sites, Δm is the change in soot mass due to the reaction [Frenklach & Wang 1994] and μ_p is the reduced soot moment. The factor α is the fraction of the surface sites available for chemical reactions; it was introduced by Frenklach and Wang [1991] to account for differences in soot surface growth rates with temperature as a result of structural changes. The functional form for α has evolved from constant values [Frenklach & Wang 1994, Colket & Hall 1994] to a temperature-dependent expression used by Appel, Bockhorn and Frenklach [2000]. Here $\alpha = \alpha_{\text{ABF00}}$, corresponding to the functional form introduced by Appel, Bockhorn and Frenklach [Appel et al. 2000] has been used. The authors are not aware of previous application of α_{ABF00} to turbulent diffusion flames.

Radiation Models In low-Mach-number flows, radiation does not alter conservation of mass, momentum and species conservation. However, the energy (absolute enthalpy) equation is modified by the presence of a radiative source term:

$$\frac{\partial \rho h}{\partial t} + \frac{\partial \rho h u_i}{\partial x_i} = -\frac{\partial J_i^h}{\partial x_i} + \frac{Dp}{Dt} + \tau_{ij}\frac{\partial u_j}{\partial x_i} + S_{\text{radiation}} \tag{5}$$

where h is the absolute enthalpy, J_i^h denotes the molecular transport of enthalpy and $S_{\text{radiation}}$ is the radiative source term interpreted as the local net volumetric gain of thermal energy due to both emission and absorption, and can be expressed as [Modest 2003]

$$S_{\text{radiation}} = -\nabla \cdot \underline{q}^R = \int_0^\infty \kappa_\eta \left(\int_{4\pi} I_\eta d\Omega - 4\pi I_{b\eta} \right) d\eta \tag{6}$$

where $\underline{q}^R$ is the radiative flux, $\kappa_\eta = \kappa_\eta(\underline{Y}, T, p)$, is the spectral absorption coefficient of the radiating medium (mixture), which may be a function of temperature T and species concentrations (expressed as mass fractions) of the radiating medium $\underline{Y}$. I_η is the spectral radiative intensity, and $I_{b\eta}$ is the Planck function or spectral blackbody intensity. The subscript η denotes spectral dependence and Ω is the solid angle.

Radiation heat transfer plays a dominant role in most industrial flames, and is governed by a complex integrodifferential equation in five dimensions [Modest 2003]. In addition, the spectral behavior of the absorption coefficient of the medium depends on its composition and local concentrations of selectively-absorbing/emitting combustion gases like water vapor, carbon dioxide and particulate matter like soot.
The simplest approximation for the radiative source term is the so-called optically thin assumption, in which local re-absorption of radiation is neglected, and spectrally integrated absorption coefficients can be used for gases and soot, resulting in a simplified expression for the radiative source term given by

$$S_{\text{radiation}} = \left(\sum_{i=1}^{i=Ngas} k_{p,i} P_i + k_{p,soot} \right) 4\sigma_{SB} \left(T^4 - T_{surr}^4 \right) \tag{7}$$

where $k_{p,i}$ is the Planck-mean absorption coefficient of radiating gases such as H_2O and CO_2, in $m^{-1}bar^{-1}$, P_i is the partial pressure of species i in bar, and $k_{p,soot}$ is the Planck-mean absorption coefficient of soot. Here we use Planck-mean, ($k_{p,soot}$), and $\kappa_{soot,\eta}$ spectral values based on Rayleigh theory [Modest 2003], assuming small particles, and a complex index of refraction based on Chang and Charalampopulous [1990]. $T_{surr} = 300\text{K}$ is used in the modeling.
For a more accurate evaluation of the radiative source term it is necessary to solve the nongray RTE, which has been done with various methods, including: i) the spherical harmonics method or a variation of it [Mazumder & Modest 1999, Li & Modest 2002]; ii) the discrete ordinates method (finite volume method) [Coelho, Teerling & Roekaerts 2003] and iii) variants based on the Photon Monte Carlo (PMC) method [Tessé et al. 2004, Snegirev 2004, Wang & Modest 2007*a*]. One powerful feature of the PMC method is that it can handle problems of high complexity with relative ease.
For a variety of combustion applications, where joint probability-density-function (PDF) methods [Pope 1985] are used, the medium is represented by notional particles evolving with time and traditional Monte Carlo ray-tracing schemes developed for continuous media are no longer useful for such stochastic media. Recently, Wang and Modest [2006] developed several emission and absorption schemes for media represented by discrete particles. The method was extended to achieve line-by-line accuracy in radiative property calculations with little increase in computational cost [Wang & Modest 2007*b*]. The PMC simulates the process of emitting radiation by releasing representative photon bundles (rays) in random directions, which are traced until they are absorbed (completely) at certain points in the medium or escape from the domain. An energy-partitioning scheme is utilized which reduces statistical error, compared to standard Monte Carlo [Modest 2003]. In media represented by discrete particles, the ray energy is distributed over all the particles that the ray interacts with, if the energy-partitioning method is employed [Wang & Modest 2006].

Turbulent Closure Transported PDF methods have been developed over the past few decades for reacting as well as nonreacting turbulent flows through the work of several researchers (see Pope [1985] and references therein). Composition PDF methods are a class of transported PDF methods, where physical scalars including temperature (or absolute enthalpy) and species concentrations are treated as random variables.
The joint PDF of these is then a function of spatial location $\underline{\mathbf{x}}$ and time t, whose transport equation can be derived [Pope 1985] and takes the form,

$$\frac{\partial \mathcal{F}}{\partial t}+\frac{\partial}{\partial x_i}[\widetilde{u}_i \mathcal{F}]+\frac{\partial}{\partial \psi_\alpha}[S_{\alpha,\mathrm{reac}}(\underline{\psi})\mathcal{F}]=-\frac{\partial}{\partial x_i}\left[\left\langle u_i'' | \underline{\psi}\right\rangle \mathcal{F}\right]+\frac{\partial}{\partial \psi_\alpha}\left[\left\langle \frac{1}{\rho}\frac{\partial J_i^\alpha}{\partial x_i} | \underline{\psi}\right\rangle \mathcal{F}\right]-\frac{\partial}{\partial \psi_\alpha}[S_{\alpha,\mathrm{rad}}(\underline{\psi})\mathcal{F}] \tag{8}$$

In Eq. (8), summation is implied over repeated indices i and α within the terms with i and α representing physical and composition space, respectively. The notation $\langle A|B\rangle$ denotes the conditional probability of event A given that B occurs. The first two terms in Eq. (8) are transport of the mass density function $\mathcal{F}$ transported with the Favre-averaged mean flow. The third term is flux in composition space due to sources that depend only on *local* composition (e.g., chemical reaction rates and radiative emission). This equation also shows that, no matter how nonlinear these sources are, they can be represented exactly. Terms on the right-hand side must be modeled. The first two terms represent transport in physical space due to turbulent diffusion and transport in composition space due to molecular-level mixing. Turbulent diffusion is commonly modeled based on the gradient-diffusion hypothesis as,

$$\left\langle u_i'' | \underline{\psi}\right\rangle \mathcal{F} \simeq \Gamma_t \frac{\partial \mathcal{F}}{\partial x_i} \tag{9}$$

The turbulent diffusivity Γ_t is estimated by an ad-hoc relationship that is derived from dimensional analysis and other considerations [Pope 1985], so that

$$\Gamma_t = C_\mu \langle \rho \rangle \sigma_\phi k^2/\varepsilon = \mu_T \sigma_\phi \tag{10}$$

where, μ_T and σ_ϕ are, respectively, the modeled turbulent diffusivity (e.g., obtained from the standard two-equation k-ε model) and a turbulent Schmidt or Prandtl number.
Various mixing models have been used to model the second term on the right-hand side of Eq. (8). In the current work, the Euclidean Minimum Spanning Tree (EMST) model by Subramaniam and Pope [1998] is used, which has been shown to perform better than other popular models in non-premixed combustion. In principle, the PDF transport Eq. (8) can be solved by traditional finite-volume and finite-element methods. This approach was used by Janicka et al. [Janicka, Kolbe & Kollmann 1978] for a jet diffusion flame. In general, however, the PDF is a function of a large number of independent variables, which makes it prohibitively expensive to use standard finite volume methods (FVM) and finite element methods (FEM). Monte Carlo approaches to the solution of the PDF equation have therefore been developed ([Pope 1985]). The basic idea is to represent the PDF by a sufficiently large number of notional fluid particles. The mean quantities at any point in the domain are then calculated as an ensemble average over the particles in a sufficiently small neighborhood. In principle, the particle tracking method is grid-free; however, in general, a grid is required to extract the statistics of the scalars at discrete locations. The algorithm presented here was developed by Pope and coworkers [Pope 1985, Muradoglu, Jenny, Pope & Caughey 1999, Jenny, Pope, Muradoglu & Caughey 2001] and by Subramaniam and Haworth [2000]. An algorithm developed by Zhang and Haworth [2004] to ensure consistency between the values obtained by a FV solution and Monte

Carlo solution is also implemented. All use a coupled flow solver to provide information about the velocity field. The numerical methods have been analyzed for different types of errors by Pope and coworkers([Xu & Pope 1999, Muradoglu, Pope & Caughey 2001]).
The third term on the right-hand side of Eq.(8) is due to radiative transfer (i.e., the difference between energy gain due absorption of incident radiation and energy loss due to local emission):

$$S_{\text{rad}} = \int_0^\infty \kappa_\eta (G_\eta - I_{b,\eta}) d\eta, \quad G_\eta = \int_{4\pi} I_\eta d\Omega, \tag{11}$$

where κ_η is the local spectral absorption coefficient, $I_{b\eta}$ is the local (spectral) blackbody intensity, and G_η is the incident radiative intensity integrated over all directions. Both κ_η and $I_{b\eta}$ are functions of local composition variables only and, therefore, local emission can be evaluated exactly using composition PDF methods. In contrast, G_η depends on properties at every (other) point in the domain and one-point PDFs are not sufficient to close the absorption term in turbulent flows. The PDF transport equation (8) is usually solved using particle Monte Carlo methods, in which the PDF is discretized into a sufficiently large number of "notional" (stochastic) particles, which are traced through the entire domain. Each particle represents a flow realization, so that the instantaneous particle field can be regarded as a snapshot of real flow [Wang & Modest 2007*a*]. Therefore, a PMC method can be employed to evaluate both the local emission ($\langle 4\pi\kappa_\eta I_{b,\eta} \rangle$) and the absorption of incident radiation ($\langle \kappa_\eta G_\eta \rangle$) exactly without any futher modeling assumptions. Emission is fundamentally closed using the one-point PDF and does not require modeling. Therefore it is evaluated correctly even when considering optically thin radiation. The PMC model allows accurate determination of both emission and absorption TRI within statistical limits and does not need any other modeling assumptions (like negligible absorption TRI etc.). Here the composition PDF method has been extended to include soot scalars (moments) as part of composition space, so that exact turbulent closure is obtained also for the highly nonlinear soot subprocesses. The required mean velocity fields in Eq. (8) are obtained using standard a k-ε model.

FLAME CONFIGURATION

A turbulent jet flame studied experimentally by Coppalle and Joyeux [1994] with a jet Reynolds number of 11,800 has been simulated. This flame has been studied numerically by Lindstedt and Louloudi [2005] using optically thin radiation. The effect of re-absorption on temperature predictions and soot yield was left as an open question. In addition, their solution method for scalar transport was a parabolic time-marching scheme, which is not generally extendable to complex configurations. Empirical models were used for all the soot subprocesses including surface growth and oxidation.
Here an elliptic solution method is employed for scalar transport (including soot moments), which can be easily applied to complex configurations. A weak co-flow is used instead of simulating a jet flame into quiescent air, and a small false pilot is employed to stabilize the flame. The jet diameter is $d_j = 4$mm with fuel velocity of 29.5m/s. A three-dimensional wedge-like grid system is employed to simulate the axisymmetric flame by applying periodic boundary conditions on the sides as shown in Fig. 1, with a wedge angle of 10°; the dimensions in x- and z- directions are $30d_j$ and $250d_j$, respectively. The grid is fine near the fuel jet to accurately resolve large local gradients in the mixing region and coarser in the coflow air region to save computational time. With composition PDF methods it is found that around 30 particles per cell on average are sufficient to resolve the turbulent fluctuations in the flame.
For radiation, following [Wang & Modest 2007*a*] the rays are traced as cones with 1° opening angles and 200,000 rays are traced per time step. Since the flames are statistically stationary, time-averaged radiative source terms evaluated for each cell are fed back to the FV code. In traditional FV methods, the residual error diminishes to zero with sufficient number of iterations, and can be used to monitor

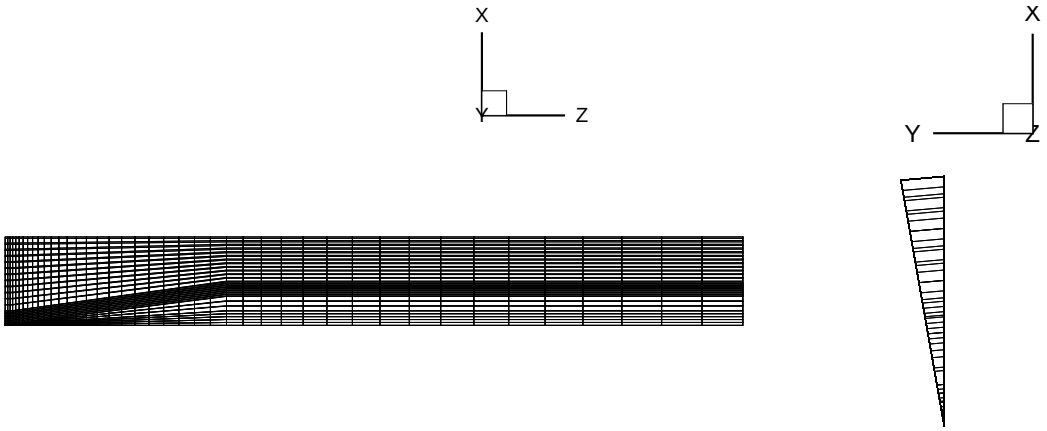

Figure 1. Grid used in simulation

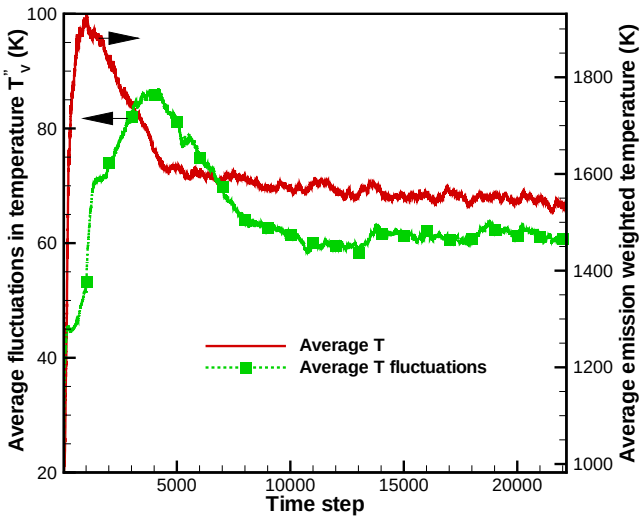

Figure 2. Progress of convergence criteria for PDF/Monte Carlo simulation

convergence. However, the residual error in hybrid FV/Monte Carlo method cannot show the same behavior due to presence of statistical noise. Hence a different metric is generally used to monitor convergence; following the approach of Wang and Modest [2007*a*], emission-weighted average temperature (T_e) and volume-averaged root-mean-square (rms) fluctuations ($\left\langle T'' \right\rangle_v$)are used to monitor convergence, i.e.,

$$T_e = \frac{\int_V k_p T^5 dV}{\int_V k_p T^4 dV} \quad \text{and} \quad \left\langle T'' \right\rangle_v = \frac{1}{V} \sum_c \left[\frac{V_c}{\rho_c} \sum_{p \in c} m_p (T_p - T_c)^2 \right]^{1/2} V_c, \tag{12}$$

where the outer sum denotes summation over cells, and the inner sum is over particles inside a cell.

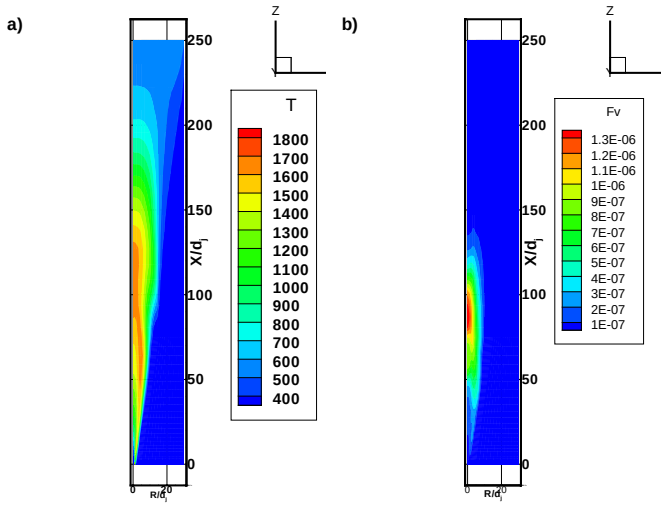

Figure 3. Mean temperature and soot volume fraction contours

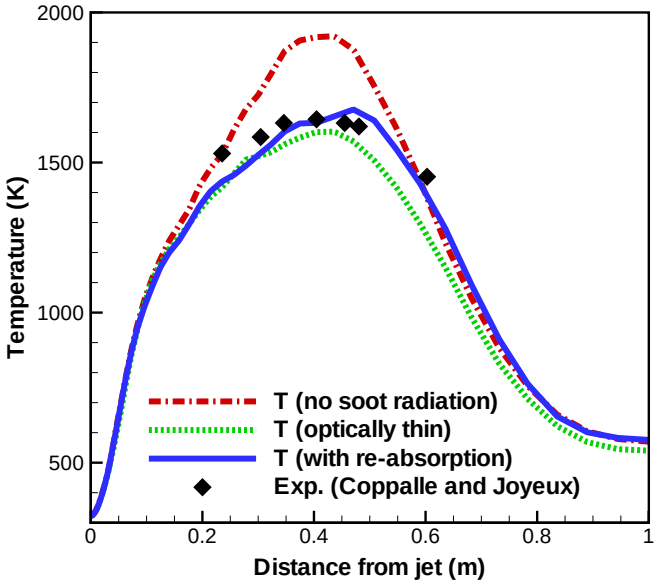

Figure 4. Measured and computed centerline mean temperature profiles using optically thin radiation and PMC method

RESULTS AND DISCUSSION

The simulations are run in a transient fashion until the convergence criteria are no longer changing with time, using a timestep of $\Delta t = 50\ \mu$s. Convergence results are shown in Fig. 2 using the PMC as RTE solver, but are similar when using the optically thin approximation. Figure 3 shows the converged steady-state contours of the mean temperature and soot volume fraction using the PMC. The contours show reasonable distribution of soot commensurate with the flame structure.

The computed centerline mean temperature profiles obtained without soot radiation, and with soot radiation using either the optically thin approximation or the PMC are shown in Fig. 4. It can be seen that soot radiation has a large effect on the temperatures and, consequently, on the entire flame structure. The peak centerline mean temperature drops by more than 300K from 1920K to 1600K in the case of optically thin radiation. Thus, optically thin radiation under-predicts peak temperature compared to the experimentally measured value of 1665K. Optically thin radiation results also under-predict temperatures in most of the downstream region. This fact has important implications on soot formation and oxidation rates, thereby changing the soot profiles. Using the PMC, (thus accounting for

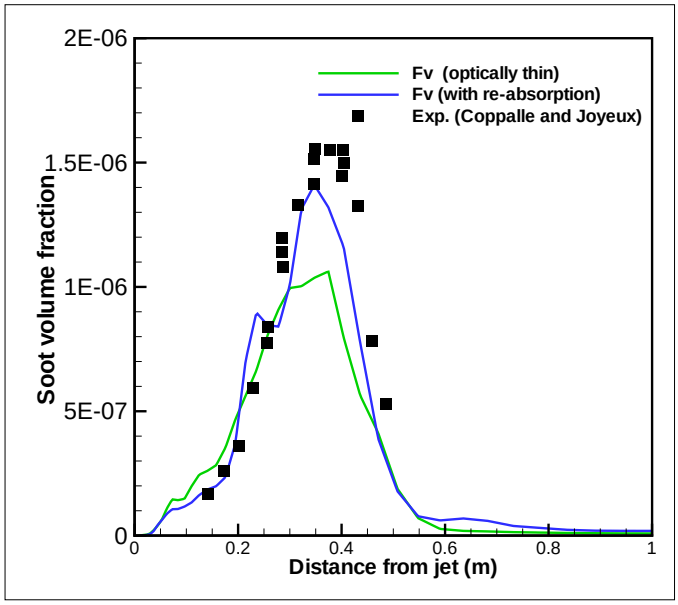

Figure 5. Measured and computed centerline mean soot volume fraction profiles using optically thin radiation and PMC method

re-absorption) results in a peak temperature of 1678K, which is closer to the experimentally reported peak axial value. Therefore, accounting for re-absorption is necessary when modeling sooting flames of this size. An important observation is that the change in temperature fields affects the soot levels, which in turn affects the amount of heat radiated from the flame.
The global (volume-integrated) emission, absorption, total heat loss and the radiant fraction (compared to chemical heat release) are listed in Table. 2. It can be seen that using the optically thin assumption, results in a higher radiant fraction and relatively low temperatures. With re-absorption, the emission is higher due to higher temperatures, but almost 15% of the emitted energy is re-absorbed in the domain. The radiant fraction is high compared to typical values found in nonsooting flames.

Table 2. Global emission, absorption and radiant fraction

Description	Total Emission (W)	Total Absorption (W)	Radiative Loss (W)	Radiant Fraction (%)
Optically Thin	6070	–	6070	28.9
PMC (with re-absorption)	6588	964	5624	26.7

The predicted centerline mean soot levels are compared with experiment in Fig. 5. It can be seen that the change in flame structure also affects the soot predictions. The peak axial soot volume fraction is slightly lower than experiments when using both optically thin and PMC models. However, considering the ppm levels of soot, the agreement is very encouraging. Re-absorption results in higher temperatures, which increase both surface growth and oxidation rates, and local conditions dictate the net effect on the soot growth rates. In the current flame accounting for re-absorption results in a higher soot formation rate, giving better agreement with experiments. Radial soot volume fractions at two different stations are shown in Fig. 6. It can be seen that predictions follow the trend of experiments. At both stations optically thin radiation model underpredicts soot to a greater extent than when accounting for re-absorption. Both models are able to capture the off-center peak location reasonably;

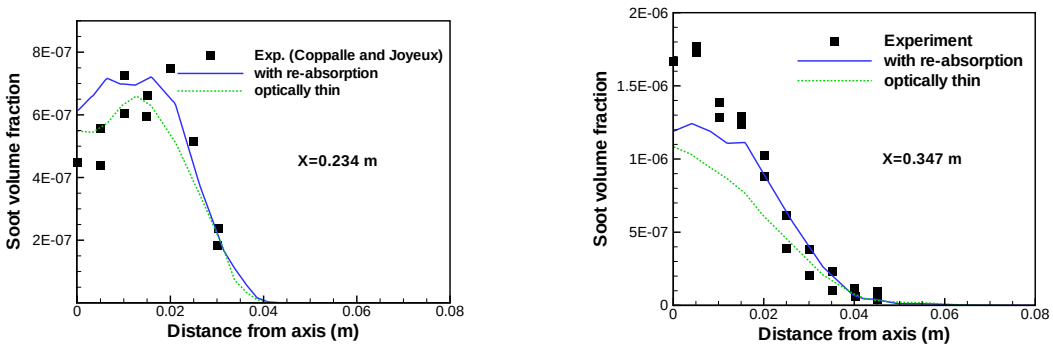

Figure 6. Measured and computed radial soot volume fraction profiles at two axial stations

agreement is better at downstream location compared to upstream.

CONCLUSION

A composition PDF method coupled with a detailed soot model was used to simulate a turbulent ethylene/air jet flame. Detailed radiation calculations were undertaken, using both optically thin radiation (neglecting re-absorption) and with spectral (nongray) photon Monte Carlo method. The effects of using different radiation models were studied based on predicted temperature and soot volume fraction profiles. It was found that accounting for re-absorption is very important in case of sooting flames. Using a composition PDF method to account for TCI accurately along with the PMC method for capturing TRI provides a powerful approach to model turbulent reacting flows, in general. The method can be extended to complex configurations and even industrial- scale problems.

Soot predictions are dependent on temperatures and vice-versa and therefore, the exact effects of TRI and TCI on the flame structure cannot be separated. Separation of the relative importance of emission TRI and absorption TRI in sooting flames has also not been undertaken. These are topics of ongoing research.

ACKNOWLEDGMENT

This work was supported by NASA under grant number NNX07AB40A.

REFERENCES

Appel, J., Bockhorn, H. & Frenklach, M. [2000], 'Kinetic moldeing of soot formation with detailed chemistry and physics: Laminar premixed flames of C_2 hydrocarbons', *Combust. Flame* **121**, 122–136.

Bandaru, R. V. [2000], Experimental Studies of the Emission Characteristics of Nonpremixed Gas-Air Flames of Various Configurations., PhD thesis, The Pennsylvania State University, University Park, PA.

Bockhorn, H. [1994], *Soot Formation in Combustion*, Springer Verlag, New York.

Chang, H. & Charalampopoulos, T. T. [1990], 'Determination of the wavelength dependence of refractive indices of flame soot', *Proceedings of the Royal Society (London) A* **430**(1880), 577–591.

Coelho, P. J. [2007], 'Numerical simulation of the interatction between turbulence and radiation in reactive flows', *Prog. Energy Combust. Sci.* **33**(4), 311–383.

Coelho, P. J., Teerling, O. J. & Roekaerts, D. [2003], 'Spectral radiative effects and turbulence/radiation interaction in a non-luminous turbulent jet diffusion flame', *Combust. Flame* **133**, 75–91.

Colket, M. B. & Hall, R. J. [1994], Successes and uncertainties in modeling soot formation in lam-

inar, premixed flames, *in* H. Bockhorn, ed., 'Soot Formation in Combustion: Mechanisms and Models', Springer-Verlag, New York.

Coppalle, A. & Joyeux, D. [1994], 'Temperature and soot volume fraction in turbulent diffusion flames: Measurements of mean and fluctuating values', *Combust. Flame* **96**, 275–285.

Cox, G. [1977], 'On radiant heat transfer from turbulent flames', *Combust. Sci. Technol.* **17**, 75–78.

Faeth, G. M., Gore, J. P., Chuech, S. G. & Jeng, S. M. [1989], Radiation from turbulent diffusion flames, *in* 'Annual Review of Numerical Fluid Mechanics and Heat Transfer', Vol. 2, Hemisphere, Washington, D.C., pp. 1–38.

Frenklach, M. [2002], 'Mehod of moments with interpolative closure', *Chemical Engineering Science* **57**, 2229–2239.

Frenklach, M. & Wang, H. [1991], 'Detailed modeling of soot particle nucleation and growth', *Proc. Combust. Inst.* **23**, 1559–1566.

Frenklach, M. & Wang, H. [1994], Detailed mechanism and modeling of soot particle formation, *in* H. Bockhorn, ed., 'Soot Formation in Combustion: Mechanisms and Models', Springer-Verlag, New York.

Fuchs, N. A. [1989], *The mechanics of aerosols*, Dover, Mineola, NY.

Harris, S. J. & Weiner, A. M. [1985], 'Chemical kinetics of soot particle growth', *Ann. Rev. Phys. Chem* **36**, 31–52.

Janicka, J., Kolbe, W. & Kollmann, W. [1978], The solution of a PDF-transport equation for turbulent diffusion flames, *in* 'Proceedings of 1978 Heat Trans. Fluid Mech. Inst., Stanford University'.

Jenny, P., Pope, S. B., Muradoglu, M. & Caughey, D. A. [2001], 'A hybrid algorithm for the joint PDF equation of turbulent reactive flows', *J. Comp. Phys.* **166**, 218–252.

Kazakov, A. & Frenklach, M. [1998], 'Dynamic modeling of soot particle coagulation and aggregation: Implementation with the method of moments and application to high-pressure laminar premixed flames', *Combust. Flame* **114**, 484–501.

Kee, R. J., Dixon-Lewis, G., Warnatz, J., Coltrin, M. E. & Miller, J. A. [1986], A computer code package for evaluation of gas-phase, multicomponent transport properties, Technical Report SAND86-8246, Sandia National Laboratory.

Kee, R. J., Rupley, F. M. & Miller, J. A. [1989], CHEMKIN-ii: A Fortran chemical kinetics package for the analysis of gas-phase chemical kinetics, Technical Report SAND89-8009B, Sandia National Laboratories.

Kennedy, I. M. [1997], 'Models of soot formation and oxidation', *Prog. Energy Combust. Sci.* **23**, 95–132.

Law, C. K. [2005], 'Comprehensive description of chemistry in combustion modeling', *Combust. Sci. Technol.* **177**, 845–870.

Leung, K. M., Lindstedt, R. P. & Jones, W. P. [1991], 'A simplified reaction mechanism for soot formation in nonpremixed flames', *Combust. Flame* **87**, 289–305.

Li, G. & Modest, M. F. [2002], 'Application of composition pdf methods in the investigation of turbulence–radiation interactions', *J. Quant. Spectrosc. Radiat. Transfer* **73**(2–5), 461–472.

Lindstedt, R. P. & Louloudi, S. A. [2005], 'Joint-scalar transported pdf modeling of soot formation and oxidation', *Proc. Combust. Inst.* **30**, 775–783.

Mazumder, S. & Modest, M. F. [1999], 'A PDF approach to modeling turbulence–radiation interactions in nonluminous flames', *Int. J. Heat Mass Transfer* **42**, 971–991.

McEnally, C., Schaffer, A., Long, M., Pfefferle, L., Smooke, M., Colket, M. & Hall, R. [1998], 'Computational and experimental study of soot formation in a coflow, laminar ethylene diffusion flame', *Proc. Combust. Inst.* **27**, 1497–1505.

Mehta, R. S., Haworth, D. C. & Modest, M. F. [2007], Composition pdf/method of moments modeling of soot formation in a turbulent ethylene/air jet flame, Fall Meeting, ESSCI, Charlottsville, VA, October 21–24, 2007.

Mehta, R. S., Haworth, D. C. & Modest, M. F. [2008], 'An assessment of gas-phase thermochemistry

and soot models for laminar atmospheric-pressure ethylene-air flames', *Proc. Combust. Inst.* . Submitted.

Modest, M. F. [2003], *Radiative Heat Transfer*, 2nd edn, Academic Press, New York.

Muradoglu, M., Jenny, P., Pope, S. B. & Caughey, D. A. [1999], 'A consistent hybrid finite volume/particle method for the PDF equations of turbulent reactive flows,', *J. Comp. Phys.* **154**, 342–371.

Muradoglu, M., Pope, S. B. & Caughey, D. [2001], 'The hybrid method for the pdf equations of turbulent reactive flows: Consistency conditions and correction algorithm', *J. Comp. Phys.* **172**, 841–878.

Neoh, K. G., Howard, J. B. & Sarofim, A. F. [1981], *in* S. D.C. & G. Smith, eds, 'Particulate Carbon: Formation During Combustion', Plenum, New York, p. 261.

Pope, S. B. [1985], 'PDF methods for turbulent reactive flows', *Prog. Energy Combust. Sci.* **11**, 119–192.

Seinfeld, J. H. & Pandis, S. N. [1998], *Atmospheric chemistry and physics. From air pollution to climate change*, Wiley, New York, NY.

Snegirev, A. Y. [2004], 'Statistical modeling of thermal radiation transfer in buoyant turbulent diffusion flames', *Combust. Flame* **136**, 51–71.

Song, T. H. & Viskanta, R. [1987], 'Interaction of radiation with turbulence: Application to a combustion system', *J. Thermoph. Heat Transfer* **1**(1), 56–62.

Subramaniam, S. & Pope, S. B. [1998], 'A mixing model for turbulent reactive flows based on euclidean minimum spanning trees', *Combust. Flame* **115**, 487–514.

Subramaniam, S. V. & Haworth, D. C. [2000], 'A PDF method for turbulent mixing and combustion on three-dimensional unstructured deforming meshes', *Intern'l. J. Engine Research* **1**, 171–190.

Tessé, L., Dupoirieux, F. & Taine, J. [2004], 'Monte carlo modeling of radiative transfer in a turbulent sooty flame', *Int. J. Heat Mass Transfer* **47**, 555–572.

Veynante, D. & Vervisch, L. [2002], 'Turbulent combustion modeling', *Prog. Energy Combust. Sci.* **28**, 193–266.

Wang, A. & Modest, M. F. [2006], 'Photon Monte Carlo simulation for radiative transfer in gaseous media represented by discrete particle fields', *J. Heat Transfer* **128**(10), 1041–1049.

Wang, A. & Modest, M. F. [2007*a*], 'Monte carlo simulation of radiative heat transfer and turbulence interactions in methane/air jet flames', *J. Quant. Spectrosc. Radiat. Transfer* **109**, 269–279.

Wang, A. & Modest, M. F. [2007*b*], 'Spectral monte carlo models for nongray radiation analyses in inhomogeneous participating media', *Int. J. Heat Mass Transfer* **50**(19-20), 3877–3889.

Wang, H., Du, D. X., Sung, C. J. & Law, C. K. [1996], 'Experiments and numerical simulation on soot formation in opposed-jet ethylene diffusion flames', *Proc. Combust. Inst.* **26**, 2359–2368.

Xu, J. & Pope, S. B. [1999], 'Assessment of numerical accuracy of PDF/Monte Carlo methods for turbulent reacting flows', *J. Comp. Phys.* **152**, 192–230.

Zhang, Y. Z. & Haworth, D. C. [2004], 'A general mass consistency algorithm for hybrid particle/finite-volume pdf methods', *J. Comp. Phys.* **194**, 156–193.